International Journal of Basic and Applied Sciences, 4 (2) (2015) 238-243
www.sciencepubco.com/index.php/IJBAS
©Science Publishing Corporation
doi: 10.14419/ijbas.v4i2.4174
Research Paper

Nanocrystalline mimetic opals: synthesis and comparative characterization vs. natural stones

M. Hernández-Ortiz [2], G. Hernández-Padrón [3], R. Bernal [4], C. Cruz-Vázquez [5], V. M. Castaño [1]*

[1] *Departamento de Ingeniería Molecular de Materiales, Centro de Física Aplicada y Tecnología Avanzada, Universidad Nacional Autónoma de México, Campus Juriquilla, Boulevard Juriquilla No. 3001, Juriquilla, Querétaro, C.P. 76230*
[2] *Facultad de Ingeniería Eléctrica, Universidad Autónoma de Zacatecas, Avenida Ramón López Velarde No. 801, 98000 Zacatecas, Zac., México*
[3] *Departamento de Nanotecnología Centro de Física Aplicada y Tecnología Avanzada, Universidad Nacional Autónoma de México, Campus Juriquilla, Boulevard Juriquilla No. 3001, Juriquilla, Querétaro, C.P. 76230*
[4] *Departamento de Investigación en Física, Universidad de Sonora, A. P. 5-088, Hermosillo, Sonora 83190 México*
[5] *Departamento de Investigación en Polímeros y Materiales, Universidad de Sonora, A. P. 130, Hermosillo, Sonora 83000 México*
**Corresponding author E-mail: meneses@unam.mx*

Abstract

The objective of this project was to synthesis and to comparative characterization of nanocrystalline opals. Synthesis technique called Stöber allows obtaining nano and micro particles monodisperse. Natural opal of origin Mexican was utilized as reference. The results obtained indicated crystalline phases in the opal, and the presence of water is shown through x-ray diffraction and the FTIR and Raman spectra, respectively. Scanning electron microscopy illustrated spherical nanoparticle of silicon. We conclude that the synthetic opal presents a mimetic character.

Keywords: *Mimetic; Morphological and Structural Characterization; Nanocrystalline; Opal; Stöber Method.*

1. Introduction

The term opal broadly includes many types of hydrated amorphous silica. It is an amorphous material in the sense that no sharp X-ray diffraction reflections are obtained, but some varieties have been shown to consist of submicroscopic crystallites of cristobalite with water between the crystals [1]. In fact, the crystal structure of opals is conventionally specified as an fcc lattice, with the direction [111] as the preferred orientation [2]. Flörke (1955) deduced that a microcrystalline opal consists of stacking disordered low-cristobalite crystallites containing structural elements of tridymite. However, in amorphous type opals, it was found that there were anomalies in the relationship between water and hydroxyl content and certain physical properties. Therefore, natural hydrated silica can be subdivided into three well defined structural groups: opal-CT, where the stacking sequence is apparently about 50% cristobalitic and 50 % tridymitic; opal-C approximately 80 to 70% cristobalitic and 20 to 30% tridymitic; and opal-A, highly disordered and nearly amorphous. Although this classification is fundamentally structural, and the water, both varies in content, and it is structurally non-essential, it is agreed in the literature that its presence in amounts greater than about 1 % is regarded as an arbitrary classification criterion [3-5].

Mono-dispersed submicron silica particles can be self-assembled into 3-dimensional periodic structures, the so-called synthetic opal. Studies on the internal structure of opal have shown the silica to form of spheres between 50 and 400 nm in diameter. Using the Stöber method it is possible to achieve excellent control of size, narrow size distribution and smooth spherical morphology of the resulting silica particles [6-9]. Moreover; it is well known that opals are converted to more highly ordered forms of cristobalite upon heating [5], [10]. In spite that there exist many reports in the literature on the synthesis of opal-like materials, scarce effort has been dedicated to mimic the nanostructure of naturally-occurring opals, which could represent an interesting venue for developing application which substitute natural opals or that enable to tailor these and other natural materials.

The ability to control the dimensions of the particles is very useful because different particle sizes are required for different applications [9], [11], [12]. For example, it has been used as a template for Si-photonic crystals with a periodic structure at the scale of the wavelength of visible-light [6]. Accordingly, the goal of this present work is to synthesize and characterize nanocrystalline opal, by controlling the formation of microstructure, aiming to mimic a natural opal, which is characterized in parallel.

2. Experimental

2.1. Synthesis process

The opal was synthesized by the Stöber method using tetraethylorthosilicate (TEOS) as the alkoxide. To carry out the hydrolysis of TEOS in an appropriate way, and to keep a controlled rate, ethanol and water and ammonium hydroxide as a catalyst for the reaction are utilized. The synthesis process consists in preparing a mixture of half concentration ethanol, deionized water and ammonium hydroxide. The solution of the remaining ethanol and TEOS was added to the alkaline solution. Molar ratios TEOS: H2O: ethanol: NH4OH, 1.8:5.5:8.75:2, respectively, were chosen to produce a particle size below 100 nm. The final mixture was continuously stirred at room temperature for 2 hours and the resulting cloudy solution was dried at 60 °C. The sample was subjected to the following heat treatments: firstly for two days at 900 °C and afterwards at 1000 ºC for one day.

2.2. Testing

X-ray diffraction (XRD) for crystalline opal was obtained in a diffractometer Rigaku, model MiniFlex +, using CuKα radiation. A FTIR spectrometer Bruker Vector 33 through the transmittance technique and Raman scattering spectroscopy, Bruker Senterra with a 785 nm laser were employed. Scanning electron microscopy (SEM) of the opal was performed in a JEOL JSM- 6060LV machine.

2.3. Natural opals

For comparison purposes, natural opals were also characterized under similar conditions. Opals used are a semiprecious stone, typical and abundant in México, extracted from the Cerro Viejo mine, near San Juan del Río, state of Queretaro. These stones are commercially known as “fire opal” [13].

3. Results and discussion

3.1 Characterization and checkout of mimetic opals

3.1.1. X-ray diffraction

After the heat treatment described above, the resulting diffraction pattern corresponds to a crystalline material with the opal-CT phase, as shown in Figure 1. Opal-CT gives an X-ray diffraction pattern with markedly broad reflections, approximately at the positions of the strong lines of cristobalite [5]. Analysis of the diffraction data by the commercial software “Materials Data Jade," reveals opal, tridymite and cristobalite phases as a good fit to identify the material.

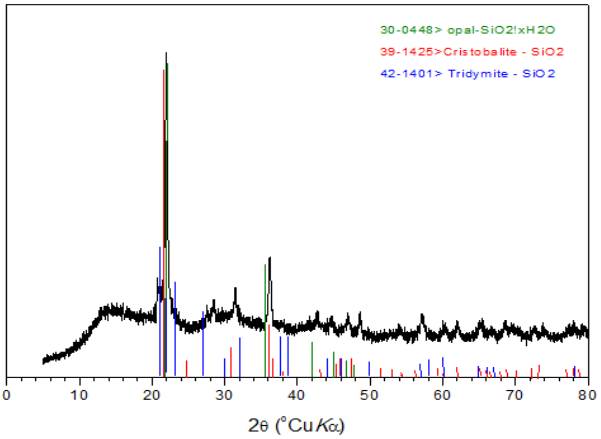

Fig. 1: X-Ray Diffraction Pattern of Synthetic Opal, Fitted to Opal, Cristobalite and Tridymite Phases.

The dominant features of the opal-CT XRD patterns are reproduced extremely well, including the shapes, positions, and widths of the 19.5-24.50 2θ band and the 35.90 2θ peak and also contain a slight shoulder on the high-2θ side of the first band [14]. Figure 2 shows those of both synthetic and natural opals.

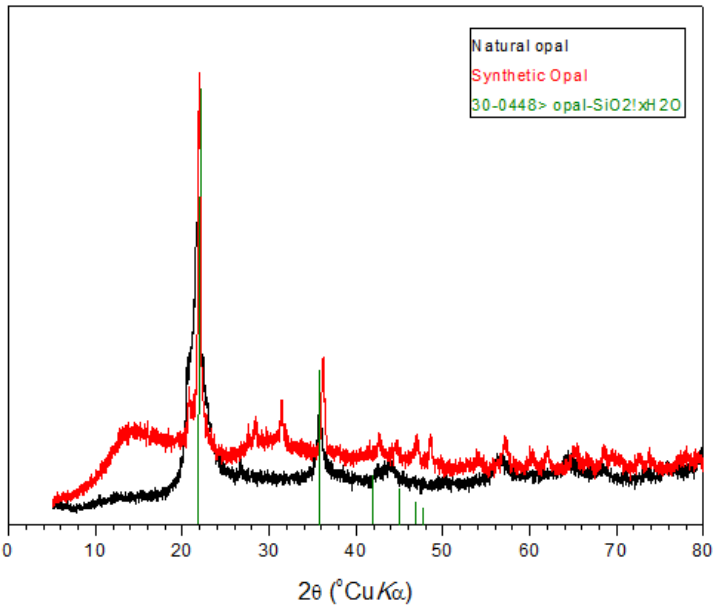

Fig. 2: X-Ray Diffraction Patterns of Both Synthetic and Natural Opals.

3.1.2. FTIR spectra

Characteristic chemical bonds in the crystalline opal were identified by the FTIR transmittance spectrum presented in Figure 3. A broad absorption band, situated at about 3500 cm-1, is assigned to the O–H stretching. Furthermore, this band can be cross checked through the 1630 cm-1 band, due to scissor bending vibration of molecular water. The absorption bands round 2900 cm-1 are C–H absorbance group and can be used to identify the presence of unreacted TEOS in the silica particles, since its intensity decreases with increasing ageing time.

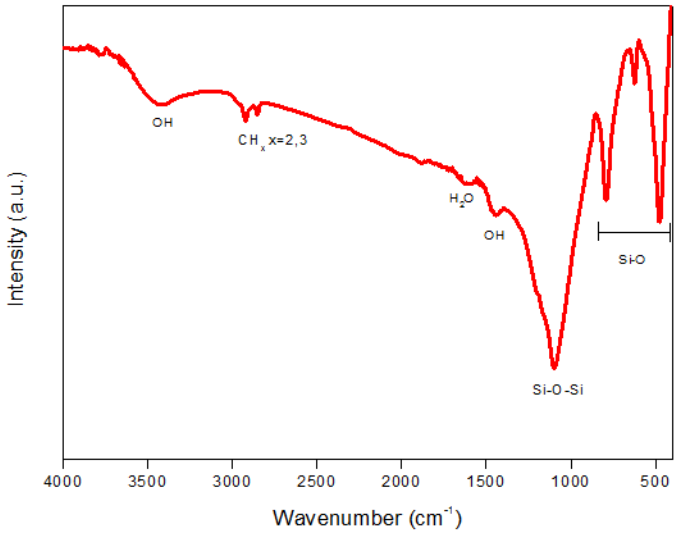

Fig. 2: FT-IR Spectroscopy of Synthetic Opal.

The major band at approximately 1100 cm-1 is assigned to the stretching vibrations of Si–O–Si or Si–O–X, where X represents ethoxy groups bonded to silicon. The shoulder at about 1200 cm-1 is assigned to either the transverse optical mode of the out of phase mode of the asymmetric vibration or to the longitudinal optical mode of the high frequency vibration of SiO2 and the symmetric vibration of Si–O is presented at 795 cm–1. The absorption band at 620 cm-1 is characteristic of low-cristobalite. Notice that it is clearly visible in the spectra of opal-C and absent for opal-CT and non-crystalline opals. Only the broad absorption band centered at 475 cm-1 is present in the opal-CT. The three absorption bands on 1100, 790 and 480 cm-1 are common to all silicates with tetrahedrally-coordinated silicon. There is very little difference between the infra-red absorption spectra of the various forms of silica in the medium-to-short wavelengths region. However, the synthetic crystalline opal obtained does not present quartz, as revealed by the distinctive absorption band in 695 cm-1, which is not present in its FTIR spectrum [3-5, 15-18]. FT-IR spectrum of fire

opal is very similar at the above case; however it does not present the absorption band at 620 cm-1, as shown in Figure 4. Hence, natural opal used in this work is part of the opal-CT structural group as described E. Fritsch et al. [13].

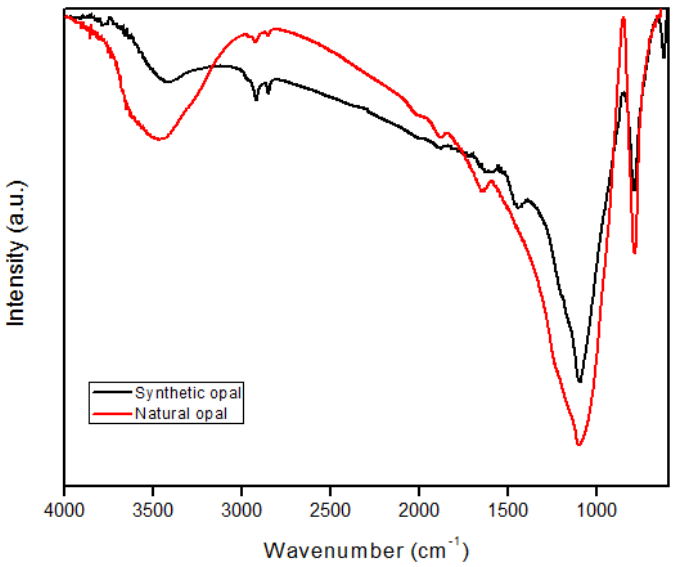

Fig. 3: Comparative FT-IR Spectra of Natural and Synthetic Opals.

3.1.3. Raman spectra

Figure 5 shows the Raman spectrum of crystalline opal after annealing. The two signals occurring about of 230 and 400 cm-1 are attributed to planar of three and four -member ring Si-O, called D1 and D2 respectively, and also the two absorption bands are assigned to normal modes of vibration of the transverse optical network (TO) and longitudinal (LO) Raman active. The Si-OH characteristic band is depicted round 800 cm-1 its intensity decreasing after of the heat treatment. Two CO2 modes at 1100 and 1300 cm-1 are observed, which indicated bending mode and symmetrical stretch, respectively. The symmetrical stretching vibration for N2 corresponding at 2321 cm-1 is not located. Raman spectrum around 3100 cm-1 is assigned to the stretching modes of CHx (x=2, 3, 4) and water molecules are given at 3300cm-1 [6], [19].

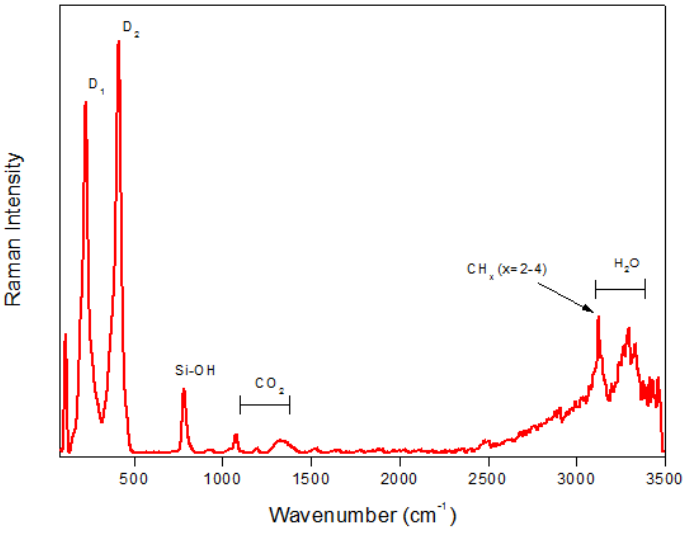

Fig. 4: Raman Spectrum of Crystalline Opal after Annealing.

Fire opal is transparent and characterized by an orange body color, hence its name. This body color originates from the light absorption by needle-like Fe3+-oxides nanoparticles (typically 10 - 100 nm) [13]. It is reason which is presented differences between Raman spectrums of natural opal and synthetic, as shown Figure 6. For example, the first absorption bands that describing rings Si-O in Raman spectrums of synthetic opal not are well defined for fire opal. Moreover, the peaks present at 550 and 650 cm-1 are characteristic of the FeO groups [20].

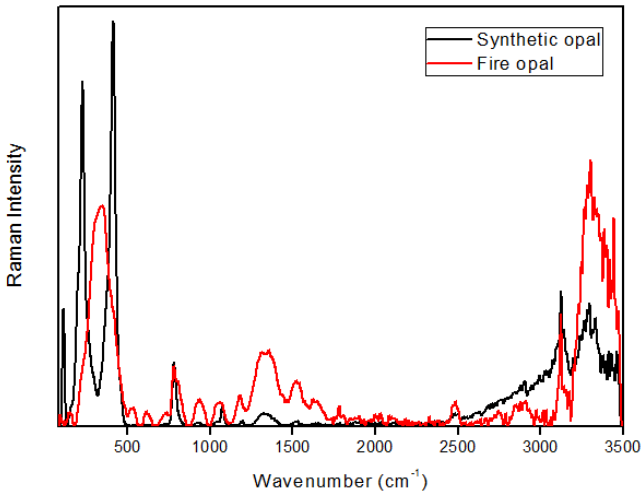

Fig. 6: Raman Spectrum of Fire Opal Compared to the Synthetic One.

3.1.4. Scanning electron microscopy

SEM image of crystalline opal in powder is displayed in Figure 7. Its average particle size is 78 nm in diameter. The spherical particles found in the natural fire opal, with average diameter of about 84 nm, are shown in Figure 8. Isolated spherical particles as well as clusters can be observed in both cases.

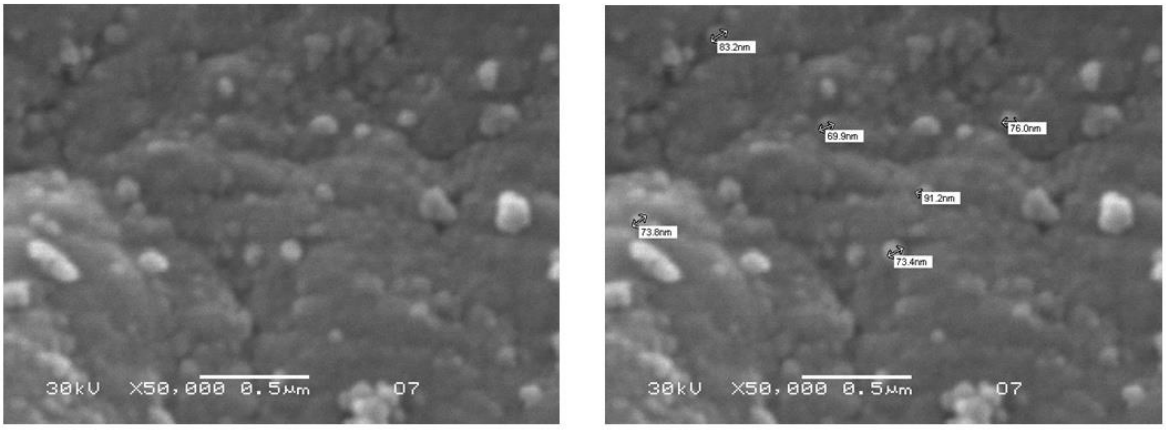

Fig. 5: Morphology of Powdered Crystalline Opal (Left). Particle Size of the Crystalline Opal (Right).

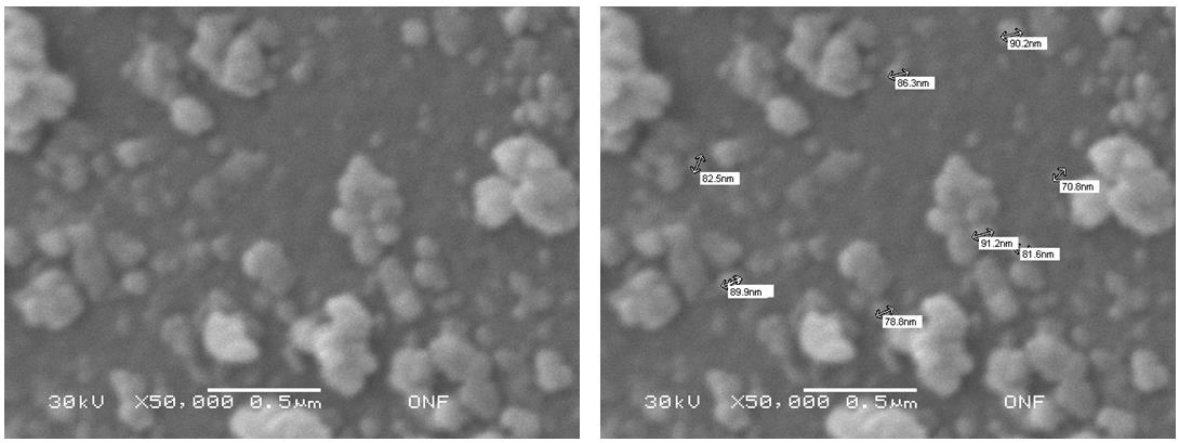

Fig. 6: SEM Images of the Fire Opal (Natural).

4. Conclusion

Crystallized synthetic opal was obtained with an average size below 100 nm. The X-ray diffraction patterns of the synthetic opal show three crystalline phases: opal, tridymite and cristobalite. FTIR spectrum indicates absence of quartz and presence of opal-C. Both spectroscopies show the existence of water in opal and of Si-O chains with tetrahedral-

coordinated silicon. The characterization of the synthetic opal does not present differences with respect to the natural opal, which reveals an interesting mimetic process.

Acknowledgement

The authors would like to thank ph. D. Marina Vega Gonzalez for technical support in the SEM studies. M. Hernández-Ortiz is a recipient of post-doctoral fellowship from CONACyT.

References

[1] R. Iler, the Chemistry of silica, John Wiley & Sons, New York, 1978; 235-297.
[2] V.G. Golubev, J.L. Hutchison, V.A. Kosobukin, et al., Three-dimensional ordered silicon-based nanostructures in opal matrix: preparation and photonic properties, Journal of Non-Crystalline Solids 1062 (2002) 299–302. http://dx.doi.org/10.1016/s0022-3093(01)01072-9.
[3] H. Graetsch, H. Gies, I. Topalović, NMR, XRD and IR study on microcrystalline opals, Physics and Chemistry of Minerals 21 (1994) 166-175. http://dx.doi.org/10.1007/BF00203147.
[4] J.B. Jones, E.R. Segnit, Water in sphere-type opal, Mineralogical Magazine 37 (1969) 357-361. http://dx.doi.org/10.1180/minmag.1969.037.287.07.
[5] J.B. Jones, E.R. Segnit, The nature of opal I. nomenclature and constituent phases, Australian Journal of Earth Sciences 18 (1971) 57-68. http://dx.doi.org/10.1080/00167617108728743.
[6] S. Inai, A. Harao, H. Nishikawa, Correlation between the luminescence properties and the surface structures of submicron silica particles, Journal of Non-Crystalline Solids 353 (2007) 510-513. http://dx.doi.org/10.1016/j.jnoncrysol.2006.10.051.
[7] W. Stöber, A. Fink, E. Bohn, Controlled Growth of Monodisperse Silica Spheres in the Micron Size Range, Journal of Colloid and Interface Science 26 (1968) 62-69. http://dx.doi.org/10.1016/0021-9797(68)90272-5.
[8] R.L. Meakins, G.J. Clark, B.L. Dikson, Thermoluminescence studies of some natural and synthetic opals, American Mineralogist 63 (1978) 737-743.
[9] L.M. Rossi, L. Shi, F.H. Quina, Z. Rosenzweig, Stöber Synthesis of Monodispersed Luminescent Silica Nanoparticles for Bioanalytical Assays, Langmuir 21 (2005) 4277-4280. http://dx.doi.org/10.1021/la0504098.
[10] M. Hernández-Ortiz, G. Hernández-Padrón, R. Bernal, C. Cruz-Vázquez, M. Vega-González, V.M. Casta-o, Nanostructured synthetic opal-C, Digest Journal of Nanomaterials and Biostructures 7 (2012) 1297-1302.
[11] M. Hernández-Ortiz, L.S. Acosta-Torres, G. Hernández-Padrón, et al., Biocompatibility of crystalline opal nanoparticles, BioMedical Engineering OnLine 11 (2012) 78-87. http://dx.doi.org/10.1186/1475-925X-11-78.
[12] M. Hernández-Ortiz, L.S. Acosta-Torres, R. Bernal, C. Cruz-Vázquez, V.M. Casta-o, Study of afterglow and thermoluminescence properties of synthetic opal-C nanoparticles for in vivo dosimetry applications, MRS Fall Proceeding 1530 (2013) mrsf12-1530-xx07-40 doi:10.1557/opl.2013.205. http://dx.doi.org/10.1557/opl.2013.205.
[13] E. Fritsch, E. Gaillou, B. Rondeau, A. Barreau, D. Albertini, M. Ostroumov, The nanostructure of fire opal, Journal of Non-Crystalline Solids 352 (2006) 3957-3960. http://dx.doi.org/10.1016/j.jnoncrysol.2006.08.005.
[14] G.D. Guthrie, D.L. Dish, R.C. Reynolds, Modeling the X-ray diffraction pattern of opal-CT, American Mineralogist 80 (1995) 869-872.
[15] G. Katumba, B.W. Mwakikunga, T.R. Mothibinyane, FTIR and Raman Spectroscopy of Carbon Nanoparticles in SiO2, ZnO and NiO Matrices, Nanoscale Research. Letters 3 (2008) 421-426. http://dx.doi.org/10.1007/s11671-008-9172-y.
[16] A. Beganskienė, V. Sirutkaitis, M. Kurtinaitienė, R. Juškėnas, A. Kareiva, FTIR, TEM and NMR Investigations of Stöber Silica Nanoparticles, Materials Science (Medžiagotyra) 10 (2004) 287-290.
[17] J.C. Chean-Wong, A. Oliver, J. Roiz, et al., Optical properties of Ir2+-implanted silica glass, Nuclear Instruments Methods in Physics Research B 175-177 (2001) 490-494. http://dx.doi.org/10.1016/S0168-583X(00)00674-1.
[18] C.K. Wu, Stable silicate glasses containing up to 10 weight percent of wáter, Journal of Non-Crystalline Solids 41 (1980) 381-398. http://dx.doi.org/10.1016/0022-3093(80)90182-9.
[19] H.Y. Zhu, R. Jianga, L. Xiao, W. Li, A novel magnetically separable γ-Fe2O3/crosslinked chitosan adsorbent: Preparation, characterization and adsorption application for removal of hazardous azo dye, Journal of Hazardous Materials 179 (2010) 251-257. http://dx.doi.org/10.1016/j.jhazmat.2010.02.087.
[20] M. Vilarigues, R.C. Da Silva, The effect of Mn, Fe and Cu ions on potash-glass corrosión, Journal of Non-Crystalline Solids 355 (2009) 1630-1637. http://dx.doi.org/10.1016/j.jnoncrysol.2009.05.051.